675

VOLUME 81 SEPARATE No. 675

PROCEEDINGS

AMERICAN SOCIETY
OF
CIVIL ENGINEERS

APRIL, 1955

PLASTIC DEFORMATIONS OF A BEAM UNDER IMPULSIVE LOADING

by B. A. Cotter and P. S. Symonds

ENGINEERING MECHANICS
DIVISION

{Discussion open until August 1, 1955}

Copyright 1955 by the AMERICAN SOCIETY OF CIVIL ENGINEERS
Printed in the United States of America

Headquarters of the Society
33 W. 39th St.
New York 18, N. Y.

PRICE $0.50 PER COPY

THIS PAPER

--represents an effort by the Society to deliver technical data direct from the author to the reader with the greatest possible speed. To this end, it has had none of the usual editing required in more formal publication procedures.

Readers are invited to submit discussion applying to current papers. For this paper the final date on which a discussion should reach the Manager of Technical Publications appears on the front cover.

Those who are planning papers or discussions for "Proceedings" will expedite Division and Committee action measurably by first studying "Publication Procedure for Technical Papers" (Proceedings – Separate No. 290). For free copies of this Separate—describing style, content, and format—address the Manager, Technical Publications, ASCE.

Reprints from this publication may be made on condition that the full title of paper, name of author, page reference, and date of publication by the Society are given.

The Society is not responsible for any statement made or opinion expressed in its publications.

This paper was published at 1745 S. State Street, Ann Arbor, Mich., by the American Society of Civil Engineers. Editorial and General Offices are at 33 West Thirty-ninth Street, New York 18, N. Y.

PLASTIC DEFORMATIONS OF A BEAM UNDER IMPULSIVE LOADING[1]

B. A. Cotter[2] and P. S. Symonds[3]

ABSTRACT

The deformation of a free-free beam subjected to a symmetric impulsive loading, specified by the initial velocity distribution of equation (1), is investigated here by means of a plastic-rigid analysis. Bleich and Salvadori discussed the same problem in a recent paper 1* [4] and presented results obtained from an elastic-plastic analysis and from a modified plastic-rigid analysis. In both analyses they assumed plastic hinge action to occur only at the center and that elsewhere the beam either deformed elastically or was rigid. The principal deformation magnitude is the final angle at the center of the beam. Results are presented here for this quantity in a general non-dimensional form, and comparisons are made with the corresponding results given by the methods used in 1*. The central angle determined by the complete plastic-rigid analysis differs markedly from that obtained by either of the "single-hinge" analyses. The range in which the complete plastic-rigid analysis can be expected to be valid is apparently different from that in which the single-hinge type of elastic-plastic analysis is accurate, the former giving reasonably good results for the central angle only when the initial velocities are sufficiently large, and the latter applying particularly to low velocities. At low velocities the single-hinge type of plastic-rigid analysis and the complete plastic-rigid solution both involve appreciable errors (in opposite directions).

INTRODUCTION

The analysis given here is based on a method developed in a previous paper 2*. A moment-curvature relation of the type shown in Fig. 1 is assumed to apply. Elastic deformations are neglected in comparison with plastic deformations. The curvature at any section is assumed constant until the moment magnitude reaches and maintains the limit moment M_o. Then the curvature may increase indefinitely, giving rise to a plastic hinge. Relative displacements of parts of the beam are assumed small enough so that changes in shape may be neglected.

We consider a free-free uniform beam of length $2l$, limit moment M_o, and mass per unit length m. The origin of the coordinate system is taken at the center of the beam with x denoting distance along the beam and y

1. The results presented in this paper were obtained in the course of research sponsored by the Office of Naval Research under Contract N7onr-35801 with Brown University.
2. Research Assistant, Division of Applied Mathematics, Brown University, Providence, R. I.
3. Professor of Engineering, Brown University, Providence, R. I.
4. Numbers with an asterisk refer to Bibliography.

displacement, as shown in Fig. 2. The beam is given an initial symmetric velocity distribution as shown in Fig. 3 described by $\frac{v_o}{2}[\,1 + \cos(\frac{\pi x}{\ell})\,]$ where v_o is a positive constant. The initial displacements are assumed zero. We are interested in finding the plastic deformation resulting from such an impulsive loading which is predicted by the plastic-rigid theory. In particular the final angle of deformation at the middle of the beam is determined; this is an important measure of the damage to the beam.

Plastic-Rigid Analysis

After the initial impact the beam undergoes translation and deformation in four different stages before deformation is completed and the beam translates as a rigid body with constant, uniform velocity. Initially the beam may be described by

$$\left.\begin{aligned} y\,(x,o) &= 0 \qquad\qquad |x| \le \ell \\ y_t\,(x,o) &= \frac{v_o}{2}\,[\,1 + \cos\,(\tfrac{\pi x}{\ell})\,] \quad |x| \le \ell \end{aligned}\right\} \qquad (1)$$

where y_t stands for $\partial y/\partial t$. The boundary conditions for a free-free beam are that the shear force and bending moment vanish at the ends. Hence

$$\left.\begin{aligned} V(\pm\,\ell, t) &= 0 \qquad t \ge 0 \\ M(\pm\,\ell, t) &= 0 \qquad t \ge 0 \end{aligned}\right\} \qquad (2)$$

where V is the shear force and M is the bending moment. It can be seen from (1) that

$$y_{xx}\,(x,o) = 0 \qquad |x| \le \ell$$

and $$y_{xxt}\,(x,o) = y_{txx}\,(x,o) = -\frac{v_o \pi^2}{2\ell^2}\cos\,(\tfrac{\pi x}{\ell}) \qquad |x| \le \ell\,.$$

Figure 4 shows the initial rate of change of curvature along the beam. Hence initially the beam has zero curvature everywhere and for $0 \le |x| < \frac{\ell}{2}$ the curvature is decreasing while for $\frac{\ell}{2} < |x| \le \ell$ the curvature is increasing. In view of the assumed moment-curvature relation of Fig. 1, and the fact that the moment and the rate of curvature must agree in sense, the <u>initial</u> moment distribution throughout the beam must be as shown in Fig. 5. In order to satisfy the boundary condition that $M(\pm\,\ell, t) = 0$ and to ensure that the bending moment is continuous along the beam, the moment distribution at a somewhat later time $t = t'$ must resemble that shown in Fig. 6.

Phase 1

Since the motion of the beam is symmetric about $x = 0$, we consider only the half beam defined by $0 \le x \le \ell$. Then at time t during the <u>first phase</u>

the configuration of the half beam is that shown in Fig. 7a. In segment I the moment is constant and equal to $-M_o$. Segments II and IV are rigid with angular velocities ω_1 and ω_2 respectively measured positively in the clockwise direction. Segment III has constant moment $+M_o$. There are plastic hinges at $x = \xi\ell$, $\eta\ell$, and $\zeta\ell$ where ξ, η, and ζ are functions of time. $\dot{\xi} < 0$, $\dot{\eta} > 0$, and $\dot{\zeta} < 0$, where $\dot{\xi}$ stands for $d\xi/dt$, so that segments I and III are diminishing in length.

The velocity in segments I and III is simply

$$y_t(x,t) = \frac{v_o}{2}\left[1 + \cos\left(\frac{\pi x}{\ell}\right)\right] \text{ for } 0 \le x < \xi\ell \text{ and } \eta\ell < x < \zeta\ell$$

since no shear forces act in these segments. In order for the transverse displacements to be continuous across the hinges, the transverse velocities must be continuous 2*. Hence

$$\left.\begin{aligned} y_t(\xi\ell+,t) &= y_t(\xi\ell-,t) = \frac{v_o}{2}\left[1 + \cos(\pi\xi)\right] \\ y_t(\eta\ell+,t) &= y_t(\eta\ell-,t) = \frac{v_o}{2}\left[1 + \cos(\pi\eta)\right] \\ y_t(\zeta\ell+,t) &= y_t(\zeta\ell-,t) = \frac{v_o}{2}\left[1 + \cos(\pi\zeta)\right] \end{aligned}\right\} \quad (3)$$

It is evident that

$$\omega_1 = \frac{y_t(\xi\ell+,t) - y_t(\eta\ell-,t)}{\ell(\eta-\xi)} = \frac{v_o}{2\ell(\eta-\xi)}\left[\cos(\pi\xi) - \cos(\pi\eta)\right] \quad (4)$$

Segment II, shown in Fig. 7b, undergoes no change in linear momentum during time t since it is not subjected to shearing forces from t = 0. Hence

$$m\int_0^{\ell(\eta-\xi)} \left[y_t(\xi\ell+,t) - \omega_1 r\right] dr = m\int_{\xi\ell}^{\eta\ell} \frac{v_o}{2}\left[1 + \cos\left(\frac{\pi x}{\ell}\right)\right] dx \quad (5)$$

Substituting the expression for $y_t(\xi\ell+,t)$ from (3) and that for ω_1 from (4) in (5) and integrating, we obtain the identity

$$(\eta-\xi)\left[\cos(\pi\xi) + \cos(\pi\eta)\right] + \frac{2}{\pi}\left[\sin(\pi\eta) - \sin(\pi\xi)\right] = 0 \quad (6)$$

External moments M_0 act on the ends of this segment during the time interval zero to t. Hence an equation can be written expression the equality of angular impulse in the time t to the change of moment of momentum of II about the point 0. Then

$$2M_0 t = m\int_0^{\ell(\eta-\xi)} [y_t(\xi\ell+,t) - \omega_1 r]r\, dr$$

$$- m\int_{\xi\ell}^{\eta\ell} \frac{v_0}{2}\left[1 + \cos\left(\frac{\pi x}{\ell}\right)\right](x-\xi\ell)dx \tag{7}$$

Using the expressions for $y_t(\xi\ell+,t)$ and ω_1 as before and integrating we obtain

$$24\,\frac{M_0}{mv_0\ell^2}\,t = \left[(\eta-\xi)^2 + \frac{6}{\pi^2}\right]\cos(\pi\xi) + \left[2(\eta-\xi)^2 - \frac{6}{\pi^2}\right]\cos(\pi\eta)$$
$$- \frac{6}{\pi}(\eta-\xi)\sin(\pi\eta). \tag{8}$$

Now (6) may be rewritten in the following form with the aid of some well-known trigonometric identities:

$$\cos\left[\frac{\pi}{2}(\xi+\eta)\right]\left\{\cos\left[\frac{\pi}{2}(\xi-\eta)\right] + \frac{2}{\pi(\xi-\eta)}\sin\left[\frac{\pi}{2}(\xi-\eta)\right]\right\} = 0 \tag{9}$$

From (9) we conclude that either

$$\cos\left[\frac{\pi}{2}(\xi-\eta)\right] + \frac{2}{\pi(\xi-\eta)}\sin\left[\frac{\pi}{2}(\xi-\eta)\right] = 0 \tag{10}$$

or

$$\cos\left[\frac{\pi}{2}(\xi+\eta)\right] = 0 \tag{11}$$

(10) yields $\xi = \eta$ which corresponds to the solution at t = 0. From (11) the identity which must hold at $t > 0$ is

$$\xi + \eta = 1. \tag{12}$$

Then (6) may be replaced by (12).
Inserting (12) in (8) gives

$$24\,\frac{M_0}{mv_0\ell^2}\,t = \left[(2\eta-1)^2 - \frac{12}{\pi^2}\right]\cos(\pi\eta) - \frac{6}{\pi}(2\eta-1)\sin(\pi\eta) \tag{13}$$

Equations (12) and (13) then give the location of two of the hinges during the first phase of the deformation.

To determine the motion of the third hinge we observe from Fig. 7c that segment IV is acted on by an external moment M_o at its end during the whole time t but is free of external forces. Since there is no change in linear momentum

$$m\int_0^{\ell(1-\zeta)} [y_t(\zeta\ell+,t) - \omega_2 r]dr = m\int_{\zeta\ell}^{\ell} \frac{v_o}{2}\left[1 + \cos\left(\frac{\pi x}{\ell}\right)\right] dx \quad (14)$$

Using the expression for $y_t(\zeta\ell+,t)$ in (3) and integrating we obtain an expression for ω_2:

$$\omega_2 \frac{\ell}{v_o} = \frac{1}{(1-\zeta)^2}\left[(1-\zeta)\cos(\pi\zeta) + \frac{1}{\pi}\sin(\pi\zeta)\right] \quad (15)$$

The equation for conservation of angular momentum, taking moments about P, becomes

$$-M_o t = m\int_0^{\ell(1-\zeta)} [y_t(\zeta\ell+,t) - \omega_2 r]r\,dr - m\int_{\zeta\ell}^{\ell} \frac{v_o}{2}\left[1 + \cos\left(\frac{\pi x}{\ell}\right)\right](x-\zeta\ell)dx \quad (16)$$

With the aid of (3), (16) reduces to

$$-12\frac{M_o}{mv_o\ell^2}t = 3\left[(1-\zeta)^2 + \frac{2}{\pi^2}\right]\cos(\pi\zeta) - 4\frac{\omega_2\ell}{v_o}(1-\zeta)^3 + \frac{6}{\pi^2} \quad (17)$$

Combining (15) and (17) gives

$$12\frac{M_o}{mv_o\ell^2}t = \left[(1-\zeta)^2 - \frac{6}{\pi^2}\right]\cos(\pi\zeta) + \frac{4}{\pi}(1-\zeta)\sin(\pi\zeta) - \frac{6}{\pi^2} \quad (18)$$

(18) then gives the location of the third hinge during the first phase.

Expressions have thus been obtained for ξ, η, and ζ as functions of t, and ω_1 and ω_2 as functions of ξ, η, and ζ during the first phase. It can be shown that $\dot{\xi} < 0$, $\dot{\eta} > 0$ and $\dot{\zeta} < 0$, so that sections I and III are diminishing in length. At some time t_1, $\eta(t_1) = \zeta(t_1)$ and $\xi(t_1) > 0$ so that III vanishes completely and the second phase of the motion begins. If we define $\xi_1 \equiv \xi(t_1)$, $\eta_1 \equiv \eta(t_1)$, and $\zeta_1 \equiv \zeta(t_1)$

then ξ_1, η_1, and ζ_1 may be determined by observing that from (12)

$$\xi_1 = 1-\eta_1 .$$

Setting $t = t_1$, and $\zeta_1 = \eta_1$ in (13) and (17), and combining gives

$$(2\eta_1^2-1)\cos(\pi\eta_1) - \frac{2}{\pi}(1 + 2\eta_1)\sin(\pi\eta_1) + \frac{12}{\pi^2} = 0 \qquad (19)$$

If (19) is solved numerically for η_1 the result is

$$\eta_1 = \zeta_1 = 0.7410$$

Then $$\xi_1 = 0.2590 \text{ and } \frac{M_o}{mv_o\ell^2} t_1 = 2.69 \times 10^{-4}$$

Phase 2

For $t > t_1$ the motion of the beam corresponds to the configuration of Fig. 9a. Section I has constant moment $-M_o$; sections II and IV are rigid with angular velocities ω_1 and ω_2 respectively, positive when measured clockwise. II and IV are separated by a moving hinge whose coordinate is $x = \eta\ell$ where $\eta = \eta(t)$. I and II are joined at a moving interface at $x = \xi\ell$, where $\xi = \xi(t)$. For this phase of the motion momentum equations cannot be written for II and IV separately since these sections have been subjected to unknown shearing forces and moments for $t > t_1$. If we define $a_1 \equiv y_{tt}(\xi\ell+,t)$ and $a_2 \equiv y_{tt}(\eta\ell+,t)$, then referring to Figs. 9b and 9c, we can write the equations of motion for II and IV respectively as follows:

$$-2M_o = \frac{1}{12} m\ell^3(\eta-\xi)^3 \dot{\omega}_1 \qquad (20a)$$

$$m\ell(\eta-\xi)\left[a_1 - \dot{\omega}_1 (\eta-\xi)\frac{\ell}{2}\right] = 0 \qquad (20b)$$

$$M_o = \frac{1}{12} m\ell^3(1-\eta)^3 \dot{\omega}_2 \qquad (21a)$$

$$m\ell(1-\eta)\left[a_2 - \dot{\omega}_2 \frac{\ell(1-\eta)}{2}\right] = 0 \qquad (21b)$$

where $\dot{\omega}_1 = \frac{d\omega_1}{dt}$ and $\dot{\omega}_2 = \frac{d\omega_2}{dt}$. Additional equations expressing the jump in transverse acceleration across the hinges at $x = \xi\ell$ and $x = \eta\ell$ may be written, as discussed in 2*.

The jump condition at the hinge at $\xi\ell$ is

$$y_{tt}(\xi\ell+,t) - y_{tt}(\xi\ell-,t) = -\dot{\xi}\ell\,[\theta_t(\xi\ell-,t) - \theta_t(\xi\ell+,t)]$$

But $$\theta_t(\xi\ell-,t) = - y_{tx}(\xi\ell-,t) = \frac{v_o}{2}\frac{\pi}{\ell}\sin(\pi\xi)$$

$$\theta_t(\xi\ell+,t) = \omega_1 \quad \text{and} \quad y_{tt}(\xi\ell-,t) = 0$$

Hence $$a_1 = - \dot{\xi}\ell\left[\frac{v_o}{2}\frac{\pi}{\ell}\sin(\pi\xi) - \omega_1\right] \tag{22}$$

The jump condition at $\eta\ell$ is

$$y_{tt}(\eta\ell+,t) - y_{tt}(\eta\ell-,t) = - \dot{\eta}\ell\left[\theta_t(\eta\ell-,t) - \theta_t(\eta\ell+,t)\right]$$

But $$y_{tt}(\eta\ell-,t) = \dot{\xi}\ell\left[\omega_1 - \frac{v_o\pi}{2\ell}\sin(\pi\xi)\right] - \dot{\omega}_1\,\ell(\eta-\xi)$$

and $$\theta_t(\eta\ell-,t) = \omega_1\ ,\ \theta_t(\eta\ell+,t) = \omega_2\ .$$

Hence

$$a_2 = \dot{\xi}\,\ell\left[\omega_1 - \frac{v_o\pi}{2\ell}\sin(\pi\xi)\right] - \dot{\omega}_1\,\ell(\eta-\xi) - \dot{\eta}\ell(\omega_1-\omega_2) \tag{23}$$

If (22) and (23) are inserted in (20b) and (21b), respectively, and the resulting expressions simplified the equations of motion become

$$\left.\begin{aligned}
(\eta-\xi)^3\,\dot{\omega}_1 &= - 24\,\frac{M_o}{m\ell^3} \\
\left(2\omega_1 - \frac{v_o\pi}{\ell}\sin(\pi\xi)\right)\dot{\xi} - (\eta-\xi)\,\dot{\omega}_1 &= 0 \\
(1-\eta)^3\,\dot{\omega}_2 &= 12\,\frac{M_o}{m\ell^3} \\
(\eta-\xi)\,\dot{\omega}_1 + 2(\omega_1-\omega_2)\,\dot{\eta} + (1-\eta)\,\dot{\omega}_2 &= 0
\end{aligned}\right\} \tag{24}$$

Thus we have to solve a set of four simultaneous first order non-linear differential equations for η, ξ, ω_1, and ω_2 as functions of t. A solution of this system can be obtained by means of numerical integration. First, however, a simplification is made in which ω_1 and ω_2 are found in terms of η, ξ, and t from momentum considerations and the resulting expressions substituted in (24).

The equation for conservation of linear momentum of the half beam for $t > t_1$ can be written

$$m\int_0^{\ell(\eta-\xi)} [y_t(\xi\ell+,t) - \omega_1 r]\, dr$$

$$+ m\int_0^{\ell(1-\eta)} [y_t(\eta\ell+,t) - \omega_2 r]\, dr$$

$$= m\int_{\xi\ell}^{\ell} \frac{v_o}{2}\left[1 + \cos\left(\frac{\pi x}{\ell}\right)\right] dx \qquad (25)$$

If we observe that $y_t(\xi\ell+,t) = \frac{v_o}{2}[1 + \cos(\pi\xi)]$

and $$y_t(\eta\ell+,t) = y_t(\xi\ell+,t) - \omega_1\ell(\eta-\xi)$$

then (25) simplifies to

$$v_o(1-\xi)\cos(\pi\xi) + \frac{v_o}{\pi}\sin(\pi\xi)$$

$$- \omega_1\ell(\eta-\xi)(2-\eta-\xi) - \omega_2\ell(1-\eta)^2 = 0 \qquad (26)$$

Since there is a moment $-M_o$ acting at x = 0 since t = 0 the equation for conservation of angular momentum for the half beam, taking moments about x = 0, becomes

$$M_o t = m\int_0^{\ell(\eta-\xi)} [y_t(\xi\ell+,t) - \omega_1 r](\xi\ell+r)\, dr$$

$$+m\int_0^{\ell(1-\eta)} [y_t(\eta\ell+,t) - \omega_2 r](\eta\ell+r)\, dr$$

$$- m\int_{\xi\ell}^{\ell} \frac{v_o}{2}\left[1 + \cos\left(\frac{\pi x}{\ell}\right)\right] x\, dx \qquad (27)$$

Completing the integration in (27) gives

$$12\,\frac{M_o}{mv_o\ell^2}\,t = 3\left(1-\xi^2+\frac{2}{\pi^2}\right)\cos(\pi\xi) - 2\,\frac{\omega_2\ell}{v_o}(1-\eta)^2(2+\eta)$$

$$- 2\,\omega_1\,\frac{\ell}{v_o}(\eta-\xi)(3-\eta^2-\xi\eta-\xi^2)$$

$$+ \frac{6}{\pi}\,\xi\,\sin(\pi\xi) + \frac{6}{\pi^2} \qquad (28)$$

Equations (26) and (28) may be used to determine ω_1 and ω_2 in terms of ξ, η, and t and the results inserted in (24). If this is done and the following change of variables made

$$y = 1-\eta\ ,\quad z = 1-\xi \text{ and } \tau = 6\,\frac{M_o}{mv_o\ell^2}\,t$$

(24) may be simplified to a pair of non-linear first order differential equations in the dependent variables z and y only, namely

$$\left.\begin{aligned}\frac{dz}{d\tau} &= \frac{2z^2}{(z-y)[\tau+\psi(z)-(z-y)\,\varphi(z)]}\\ \frac{dy}{d\tau} &= \frac{(z-y)^2-2y^2}{(z-y)(\tau+\psi(z))}\end{aligned}\right\} \qquad (29)$$

where $\psi(z) = \frac{1}{2}\left(\frac{6}{\pi^2}-z^2\right)\cos(\pi z) + \frac{2}{\pi}\,z\,\sin(\pi z) - \frac{3}{\pi^2}$

and $\varphi(z) = z\,\cos(\pi z) + \frac{\pi}{2}\left(z^2-\frac{2}{\pi^2}\right)\sin(\pi z)$

The differential equations (29) were integrated numerically using as initial conditions the values obtained for ξ, η, and t at the end of phase 1, namely

$$y_1 = 1-\eta_1 = .2590 \qquad z_1 = 1-\xi_1 = .7410$$

$$\tau_1 = 6\,\frac{M_o}{mv_o\ell^2}\,t_1 = 1.614 \times 10^{-3}$$

Initial values of y_1 and z_1 in the integration were obtained by the Kutta-Simpson rule applied to a system of two first-order differential equations 3*. Then the integration was completed over the required range by one of the standard methods of forward integration. The results of the integration show that $\eta < 0$ and $\xi < 0$ for this phase so that the interface at $x = \xi\ell$ and the hinge at $x = \eta\ell$ are moving toward the center of the beam. At time

$t = t_2$ the angular velocities ω_1 and ω_2 become equal while ξ is still positive, indicating the disappearance of the hinge at $x = \eta \ell$. This concludes the second phase of the motion. If we define $\xi(t_2) = \xi_2$ and $\eta(t_2) = \eta_2$ it is found that

$$\xi_2 = .1498 \qquad \eta_2 = .6469 \qquad \text{and} \qquad \frac{M_o}{mv_o\ell^2}\, t_2 = .001216$$

Phase 3

For $t > t_2$ the beam consists of a rigid segment with angular velocity and a plastic segment with constant moment $-M_o$. These are separated by a moving interface with coordinate $x = \xi\ell$ as shown in Fig. 10. A moment $-M_o$ still acts at $x = 0$. Momentum considerations may again be invoked to describe the motion of the beam in this phase. Since no external forces act on the half beam conservation of linear momentum gives

$$m\int_0^{\ell(1-\xi)} [\, y_t(\xi\ell+,t) - \omega x]\, dx = m\int_{\xi\ell}^{\ell} \frac{v_o}{2}\left[1 + \cos\left(\frac{\pi x}{\ell}\right)\right] dx \tag{30}$$

where $$y_t(\xi\ell+,t) = \frac{v_o}{2}\left[1 + \cos(\pi\xi)\right].$$

If the integration in (30) is carried out the result is

$$\frac{\omega\ell}{v_o} = \frac{1}{(1-\xi)^2}\left[(1-\xi)\cos(\pi\xi) + \frac{1}{\pi}\sin(\pi\xi)\right] \tag{31}$$

Conservation of angular momentum, taking moments about $x = 0$, gives

$$M_o t = \int_0^{\ell(1-\xi)} m[y_t(\xi\ell+,t) - \omega x](\xi\ell+x)\, dx - \int_{\xi\ell}^{\ell} m\,\frac{v_o}{2}\left[1 + \cos\left(\frac{\pi x}{\ell}\right)\right] x\, dx \tag{32}$$

With the value of ω from (31), equation (32) reduces to

$$12\,\frac{M_o}{mv_o\ell^2}\, t = \left[\frac{6}{\pi^2} - (1-\xi)^2\right]\cos(\pi\xi) - \frac{4}{\pi}(1-\xi)\sin(\pi\xi) + \frac{6}{\pi^2} \tag{33}$$

(33) gives the location of the moving hinge for $t > t_2$. It can be shown that $\dot{\xi} < 0$ for this phase so that section I is diminishing in length. At some time t_3, $\xi = 0$ and the half beam becomes entirely rigid with a hinge at $x = 0$. t_3 is simply determined by setting $\xi = 0$ in equation (33). Then

$\frac{M_o}{mv_o\ell^2} t_3 = \frac{1}{\pi^2} - \frac{1}{12}$. This concludes the third phase.

Phase 4

For $t > t_3$ the half-beam is rigid and moves as if hinged at the point $x = 0$ as shown in Fig. 11. Here the bending moment is $-M_o$ and if the angular velocity of the half-beam is ω we may write the angular momentum equation, taking moments about $x = 0$, as follows:

$$M_o t = m \int_o^\ell [y_t(o,t) - \omega x] x \, dx - m \int_o^\ell \frac{v_o}{2} [1 + \cos(\frac{\pi x}{\ell})] x \, dx \tag{34}$$

We observe that $y_t(o,t)$ is unknown for this phase. (34) reduces upon integrating to

$$6 \frac{M_o}{mv_o\ell^2} t = 3 \frac{y_t(o,t)}{v_o} - 2 \frac{\omega\ell}{v_o} - \frac{3}{2} + \frac{6}{\pi^2} \tag{35}$$

Conservation of linear momentum of the half-beam yields

$$m \int_o^\ell [y_t(o,t) - \omega x] \, dx = m \int_o^\ell \frac{v_o}{2} [1 + \cos(\frac{\pi x}{\ell})] \, dx \tag{36}$$

From (36) an expression is obtained for $y_t(o,t)$, namely

$$y_t(o,t) = \frac{v_o}{2} (1 + \frac{\omega\ell}{v_o}) \tag{37}$$

If (37) and (35) are combined the result is an expression for the angular velocity ω as a function of time

$$\frac{\omega\ell}{v_o} = 12 (\frac{1}{\pi^2} - \frac{M_o}{mv_o\ell^2} t) \tag{38}$$

The beam continues to translate and rotate with angular velocity ω until some time $t = t_4$ when $\omega = 0$. From (38)

$$\frac{M_o}{mv_o\ell^2} t_4 = \frac{1}{\pi^2} \tag{39}$$

At $t = t_4$ deformation of the beam is completed and for $t > t_4$ the entire beam translates as a rigid body with constant velocity. The final transverse velocity v_f of the beam results from setting $\omega = 0$ in (37) and is found to be $\frac{v_o}{2}$.

As a check, the same result is found directly by equating the initial linear

momentum $m\ell v_o$ of the beam to the linear momentum in the final phase of rigid body translation, namely $2m\ell v_f$.

Deformation at the Middle

The angle of deformation at the middle of the beam may now be calculated quite readily. First observe that for $0 < t < t_3$

$$y_t(x,t) = \frac{v_o}{2}\left[1 + \cos\left(\frac{\pi x}{\ell}\right)\right] \quad \text{for } 0 \le x \le \xi\ell$$

and hence $$y_{xt}(x,t) = -\theta_t(x,t) = -\frac{v_o}{2}\frac{\pi}{\ell}\sin\left(\frac{\pi x}{\ell}\right)$$

Then the angle of deformation at the middle of the beam for $0 \le t \le t_3$ is simply $\theta(o,t) = 0$. For $t_3 < t < t_4$

$$\theta(o+,t) = \int_{t_3}^{t} \omega dt' = \frac{12v_o}{\ell}\int_{t_3}^{t}\left(\frac{1}{\pi^2} - \frac{M_o}{mv_o\ell^2}\,t'\right)dt'$$

Then $$\frac{M_o}{mv_o^2\ell}\,\theta(o+,t) = \frac{1}{24} - 6\left(\frac{M_o}{mv_o\ell^2}\,t - \frac{1}{\pi^2}\right)^2$$

Since at $t = t_4$ deformation ceases, the final angle $\theta(o+,t_4) = \theta_{of}$ of deformation at the middle is

$$\frac{M_o}{mv_o^2\ell}\,\theta_{of} = \frac{1}{24}\,.$$

To summarize, then, if $\theta(o+,t) = \theta_o(t)$,

$$\frac{M_o}{mv_o^2\ell}\,\theta_o(t) = \begin{cases} 0 & 0 \le t \le t_3 \\ \frac{1}{24} - 6\left(\frac{M_o}{mv_o\ell^2}\,t - \frac{1}{\pi^2}\right)^2 & t_3 \le t \le t_4 \\ \frac{1}{24} & t > t_4 \end{cases} \tag{40}$$

Figure 12 shows a plot of the non-dimensional quantity $\frac{M_o}{mv_o^2\ell}\,\theta_o(t)$ as a function of the non-dimensional time $\frac{M_o}{mv_o\ell^2}\,t$.

Energy Check

An overall check on the results obtained in this analysis is available through energy considerations. The initial kinetic energy of the beam is

easily calculated and is found to be $\frac{3}{8}\, m\ell v_o^2$. The final kinetic energy of the deformed beam is $\frac{1}{4}\, m\ell v_o^2$; this is obtained from considerations of momentum conservation. Hence the loss of kinetic energy is $\frac{1}{8}\, m\ell v_o^2$. This must be equal to the plastic work done on the beam during deformation, W_p, which is given by

$$W_p = 2\,[M_o\theta_{of} + M_o(\theta_{mf} - \theta_{of}) + M_o(\theta_{mf} - \theta_{1f})]$$

$$= 4M_o\theta_{mf} - 2M_o\theta_{1f}$$

where $\theta_{mf} = \theta(\frac{\ell}{2}, t_f)$, and $\theta_{1f} = \theta(\ell, t_f)$. θ_{mf} and θ_{1f} may be found by direct integration over the entire range $0 \le t \le t_f$ with the exception of phase 2 during which the integration must be performed numerically. If this is done the result is $\theta_{mf} = .0621\, \frac{m\ell v_o^2}{M_o}$ and $\theta_{1f} = .0616\, \frac{m\ell v_o^2}{M_o}$. Then $W_p = .1252\; m\ell v_o^2$ which agrees within the accuracy of the calculations with the loss in kinetic energy.

Discussion of Results

We observe that, since all deformation at the midpoint takes place during phase 4, $\theta_o(t)$ may be calculated from the motion of this phase once the value of t_3 has been obtained from the solution of phase 3. Hence it appears that θ_{of} may be determined without obtaining a solution for the first two configurations thereby obviating the need for resorting to numerical integration. However, in order to ensure that no phases of the type shown in Fig. 13a and 13b occur in place of 2 and 3, it is necessary to determine the motion for these two phases. If the configurations of Fig. 13 were to apply the central angle $\theta_o(t)$ would not be easily calculable.

A comparison may be made between the present results and those obtained by Bleich and Salvadori in 1*. They obtain midpoint angles of deformation for a specific beam with m = .800, ℓ = 160, $M_o = 6.69 \times 10^4$, and EI = 3.58×10^8 for two values of v_o, namely v_o = 11.1, and v_o = 67.4. Their results for the two cases appear in Table I together with values of $\theta_o(t)$ obtained by the correct rigid-plastic analysis developed here. θ_e is obtained in 1* by an elastic-plastic analysis in which the limit moment M_o is assumed to occur only at the mid-point at an "initial plasticity time," t_o. θ_u is the result determined in 1* by assuming the beam hinged at the middle and rigid elsewhere from t = 0 until deformation is completed. θ_ℓ is obtained from the same "single-hinge" assumption for $t > t_o$ with the beam elastic for $0 \le t < t_o$. Since the angles of deformation reported in 1* are defined to be equal to the discontinuity in slope:

$$\theta(t) = y_x(o+, t) - y_x(o-, t)$$

the quantities θ_u, θ_ℓ, and θ_e have, by definition, twice the magnitude of the central angles discussed in the present analysis. Hence in Table I we compare $2\theta_o$ with θ_u, θ_ℓ, and θ_e.

If we employ the criterion for the validity of the plastic-rigid analysis suggested in 2*, namely that the plastic work done on the beam, W_p, be much greater than the maximum elastic energy $\frac{M_o 2\ell}{EI}$, then, if $R = \frac{W_p}{M_o 2\ell/EI}$, our results should be valid for $R >> 1$. For $v_o = 11.1$, $R = .986$ and for $v_o = 67.4$, $R = 36.3$. Thus we might expect θ_{of} to be approximately correct for the higher value of v_o only. However, Table I indicates marked differences between θ_{of} and the final angles obtained by either of the "single-hinge" analyses for $v_o = 67.4$; the final angle of deformation which is predicted by the three different analyses in 1* is about 50% higher than that yielded by the rigid-plastic solution. For $v_o = 11.1$, $R \sim 1$ so that the value of θ_{of} obtained in this case is not expected to be valid. However, the results of the single-hinge elastic-plastic solution are probably accurate here. For this velocity the positive error of the single-hinge plastic-rigid solution has about the same magnitude as the negative error of the complete plastic-rigid solution.

It should be noted that the disagreement between the elastic-plastic and the present rigid-plastic solution at the higher velocity v_o - 67.4 does not mean that the latter solution must be in error. In fact, the agreement between the elastic-plastic solution and the single-hinge rigid-plastic solution is an indication that the elastic-plastic solution is inaccurate at this velocity because it takes account of plastic flow solely at the mid-section. Such agreement between the two "single-hinge" solutions is to be expected at sufficiently high velocities, if these are regarded as the correct solution for a problem of a fictitious beam whose yield stress varies along the beam so that plastic flow at the limit moment M_o occurs only at the middle. Both solutions are presumably incorrect for the uniform beam problem. The complete plastic-rigid analysis of this paper may well be accurate at the higher velocity, but confirmation by comparison with a complete elastic-plastic solution still remains to be obtained.

In an oral communication based on an advance copy of the present paper Professor Bleich has called attention to the interest of a comparison between the final angle at the mid-point determined by the elasto-plastic analysis of 1* and the total angle across the central plastic zone in the complete plastic-rigid analysis. In the latter solution there is a zone of length ℓ with negative permanent curvature occupying the middle portion of the beam, while the two outer quarters have positive curvature. The total angle between the tangents at the two ends of the negative zone is $2\theta_{mf} = 0.1242\, m\ell v_o^2/M_o$. For the two cases treated numerically in 1* the final values of the relative angle across the entire negative plastic zone of length ℓ are:

$$v_o = 11.1 \qquad\qquad v_o = 67.4$$

$$\frac{2\theta_{mf}}{v_o} \times 10^3 = 2.64 \qquad\qquad \frac{2\theta_{mf}}{v_o} \times 10^2 = 1.60 \,.$$

The very close agreement of these results with the corresponding values (2.63, 1.58) of the single-hinge rigid-plastic solution is natural in view of the fact that the work done in positive plastic deformation (in the outer quarters of the beam) is less than one percent of the work done in producing negative plastic deformation; this is shown by the figures given on p. 17.

As far as damage to the beam is concerned the angle of slope discontinuity at a plastic hinge is especially significant. At any plastic hinge there must of course be a small but finite plastic zone in a physical beam, since a slope discontinuity would imply infinite strains. Such a smoothing out of the theoretical angle of discontinuity would occur at the central hinge predicted either by the elasto-plastic analysis of 1* or by the present plastic-rigid analysis. The comparisons between central angles shown in Table I appear therefore to be of primary interest in assessing the various methods.

REFERENCES

1. "Impulsive Motion of Elasto-Plastic Beams," by H. H. Bleich and M. G. Salvadori, Proceedings ASCE, Separate No. 287, Vol. 79, 1953.
2. "Large Plastic Deformations of Beams under Transverse Impact," by E. H. Lee and P. S. Symonds, Trans. ASME, Vol. 74, 1952, p. 308.
3. "Numerical Solutions of Differential Equations," by H. Levy and E. A. Baggott, pp. 106, 160.

Table I

ANGLE OF DEFORMATION AT MID-POINT OF FREE-FREE BEAM

	$v_o = 11.1$				$v_o = 67.4$		
t	$\frac{2\theta_o}{v_o} \times 10^3$	$\frac{\theta_u}{v_o} \times 10^3$	$\frac{\theta_e}{v_o} \times 10^3$	$\frac{\theta_\ell}{v_o} \times 10^3$	t	$\frac{2\theta_o}{v_o} \times 10^2$	$\frac{\theta_u}{v_o}$, $\frac{\theta_e}{v_o}$, $\frac{\theta_\ell}{v_o} \times 10^2$
0	0	0	0	0	0	0	0
.05	0	.66	0	0	.25	0	.36
.061	0	.73	0	0	.50	.152	.68
.10	.450	1.30	0	0	.75	.421	.93
.15	.932	1.80	0	0	1.0	.640	1.16
.20	1.310	2.18	0	0	1.25	.818	1.32
.25	1.574	2.44	.54	.40	1.50	.948	1.46
.30	1.724	2.57	1.38	.68	1.75	1.035	1.53
.35	1.770	2.63	1.97	.84	2.0	1.073	1.56
.40	↓	2.63	2.20	.93	2.25	1.075	1.58
.45	↓	↓	↓	.95		↓	↓
				↓			

θ_o - Correct Plastic-Rigid Solution

θ_u - Upper Bound Solution

θ_e - Elastic-Plastic Solution } Bleich and Salvadori

θ_ℓ - Lower Bound Solution

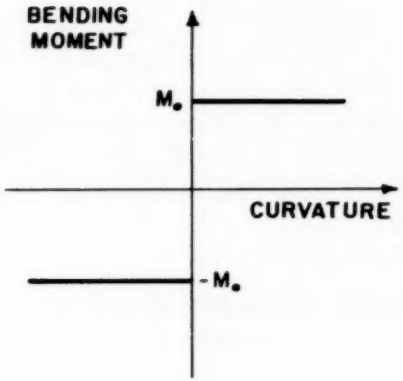

Fig. 1

ASSUMED MOMENT-CURVATURE RELATION

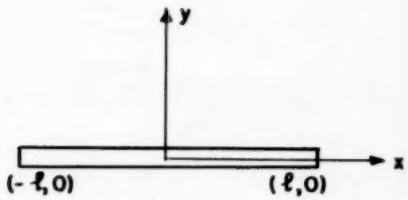

Fig. 2

UNIFORM BEAM AT $t = 0$

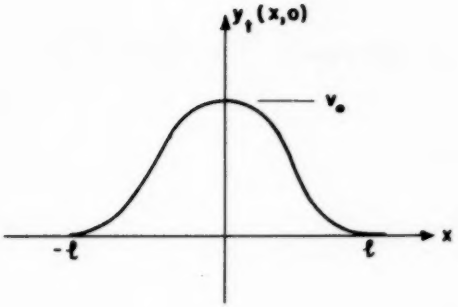

Fig. 3

INITIAL VELOCITY DISTRIBUTION

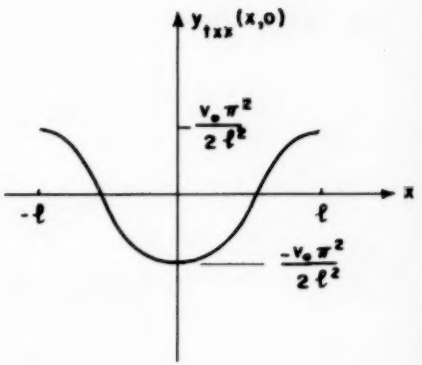

Fig. 4

INITIAL RATE OF CHANGE OF CURVATURE

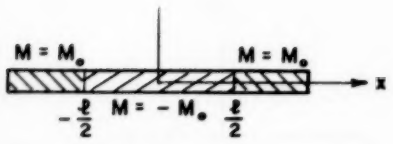

Fig. 5

MOMENT DISTRIBUTION JUST AFTER t=0.

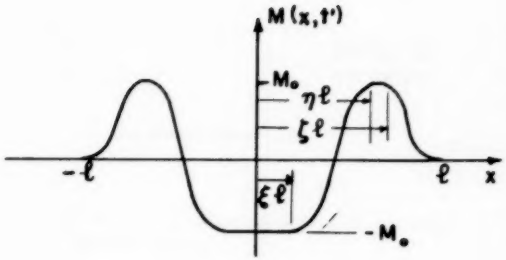

Fig. 6

MOMENT DISTRIBUTION DURING PHASE I

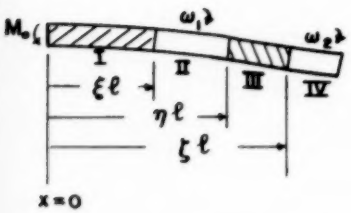

a: HALF BEAM

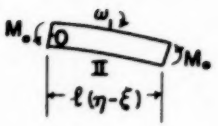

b: SECTION II

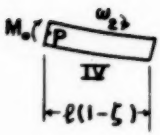

c: SECTION IV

Fig. 7

PHASE I. $0<t<t_1$

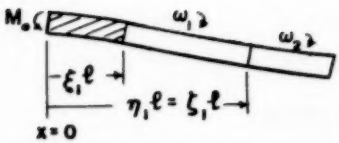

Fig. 8

HALF BEAM AT $t=t_1$

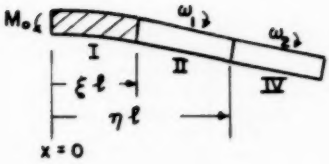

a: HALF BEAM

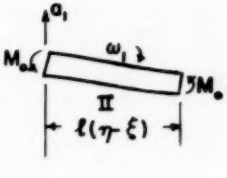

b: SECTION II

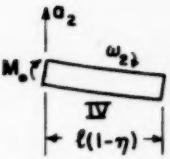

c: SECTION IV

Fig. 9

PHASE 2. $t_1 < t < t_2$

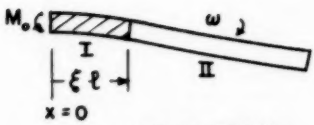

HALF BEAM

Fig. 10

PHASE 3 $t_2 < t < t_3$

HALF BEAM

Fig. 11

PHASE 4 $t_3 < t < t_4$

(a)

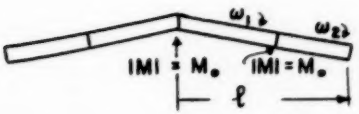

(b)

Fig. 13

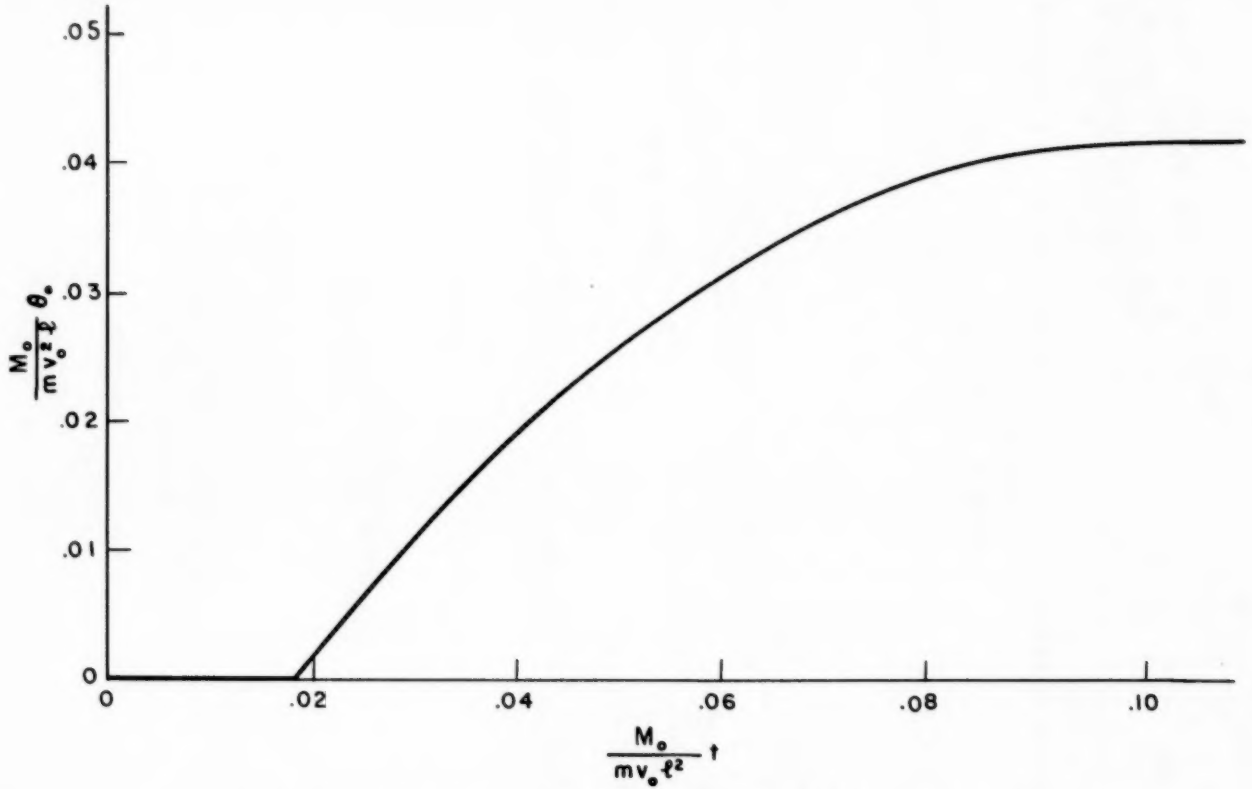

Fig. 12. VARIATION OF ANGLE OF DEFORMATION AT MIDDLE WITH TIME

PROCEEDINGS-SEPARATES

The technical papers published in the past year are presented below. Technical-division sponsorship is indicated by an abbreviation at the end of each Separate Number, the symbols referring to: Air Transport (AT), City Planning (CP), Construction (CO), Engineering Mechanics (EM), Highway (HW), Hydraulics (HY), Irrigation and Drainage (IR), Power (PO), Sanitary Engineering (SA), Soil Mechanics and Foundations (SM), Structural (ST), Surveying and Mapping (SU), and Waterways (WW) divisions. For titles and order coupons, refer to the appropriate issue of "Civil Engineering" or write for a cumulative price list.

VOLUME 80 (1954)

APRIL: 428(HY)[c], 429(EM)[c], 430(ST), 431(HY), 432(HY), 433(HY), 434(ST).

MAY: 435(SM), 436(CP)[c], 437(HY)[c], 438(HY), 439(HY), 440(ST), 441(ST), 442(SA), 443(SA).

JUNE: 444(SM)[e], 445(SM)[e], 446(ST)[e], 447(ST)[e], 448(ST)[e], 449(ST)[e], 450(ST)[e], 451(ST)[e], 452(SA)[e], 453(SA)[e], 454(SA)[e], 455(SA)[e], 456(SM)[e].

JULY: 457(AT), 458(AT), 459(AT)[c], 460(IR), 461(IR), 462(IR), 463(IR)[c], 464(PO), 465(PO)[c].

AUGUST: 466(HY), 467(HY), 468(ST), 469(ST), 470(ST), 471(SA), 472(SA), 473(SA), 474(SA), 475(SM), 476(SM), 477(SM), 478(SM)[c], 479(HY)[c], 480(ST)[c], 481(SA)[c], 482(HY), 483(HY).

SEPTEMBER: 484(ST), 485(ST), 486(ST), 487(CP)[c], 488(ST)[c], 489(HY), 490(HY), 491(HY)[c], 492(SA), 493(SA), 494(SA), 495(SA), 496(SA), 497(SA), 498(SA), 499(HW), 500(HW), 501(HW)[c], 502(WW), 503(WW), 504(WW)[c], 505(CO), 506(CO)[c], 507(CP), 508(CP), 509(CP), 510(CP), 511(CP).

OCTOBER: 512(SM), 513(SM), 514(SM), 515(SM), 516(SM), 517(PO), 518(SM)[c], 519(IR), 520(IR), 521(IR), 522(IR)[c], 523(AT)[c], 524(SU), 525(SU)[c], 526(EM), 527(EM), 528(EM), 529(EM), 530(EM)[c], 531(EM), 532(EM)[c], 533(PO).

NOVEMBER: 534(HY), 535(HY), 536(HY), 537(HY), 538(HY)[c], 539(ST), 540(ST), 541(ST), 542(ST), 543(ST), 544(ST), 545(SA), 546(SA), 547(SA), 548(SM), 549(SM), 550(SM), 551(SM), 552(SA), 553(SM)[c], 554(SA), 555(SA), 556(SA), 557(SA).

DECEMBER: 558(ST), 559(ST), 560(ST), 561(ST), 562(ST), 563(ST)[c], 564(HY), 565(HY), 566(HY), 567(HY), 568(HY)[c], 569(SM), 570(SM), 571(SM), 572(SM)[c], 573(SM)[c], 574(SU), 575(SU), 576(SU), 577(SU), 578(HY), 579(ST), 580(SU), 581(SU), 582(Index).

VOLUME 81 (1955)

JANUARY: 583(ST), 584(ST), 585(ST), 586(ST), 587(ST), 588(ST), 589(ST)[c], 590(SA), 591(SA), 592(SA), 593(SA), 594(SA), 595(SA)[c], 596(HW), 597(HW), 598(HW)[c], 599(CP), 600(CP), 601(CP), 602(CP), 603(CP), 604(EM), 605(EM), 606(EM)[c], 607(EM).

FEBRUARY: 608(WW), 609(WW), 610(WW), 611(WW), 612(WW), 613(WW), 614(WW), 615(WW), 616(WW), 617(IR), 618(IR), 619(IR), 620(IR), 621(IR)[c], 622(IR), 623(IR), 624(HY)[c], 625(HY), 626(HY), 627(HY), 628(HY), 629(HY), 630(HY), 631(HY), 632(CO), 633(CO).

MARCH: 634(PO), 635(PO), 636(PO), 637(PO), 638(PO), 639(PO), 640(PO), 641(PO)[c], 642(SA), 643(SA), 644(SA), 645(SA), 646(SA), 647(SA)[c], 648(ST), 649(ST), 650(ST), 651(ST), 652(ST), 653(ST), 654(ST)[c], 655(SA), 656(SM)[c], 657(SM)[c], 658(SM)[c].

APRIL: 659(ST), 660(ST), 661(ST)[c], 662(ST), 663(ST), 664(ST)[c], 665(HY)[c], 666(HY), 667(HY), 668(HY), 669(HY), 670(EM), 671(EM), 672(EM), 673(EM), 674(EM), 675(EM), 676(EM), 677(EM), 678(HY).

c. Discussion of several papers, grouped by Divisions.
e. Presented at the Atlantic City (N.J.) Convention in June, 1954.

AMERICAN SOCIETY OF CIVIL ENGINEERS

OFFICERS FOR 1955

PRESIDENT

WILLIAM ROY GLIDDEN

VICE-PRESIDENTS

Term expires October, 1955:
ENOCH R. NEEDLES
MASON G. LOCKWOOD

Term expires October, 1956:
FRANK L. WEAVER
LOUIS R. HOWSON

DIRECTORS

Term expires October, 1955:
CHARLES B. MOLINEAUX
MERCEL J. SHELTON
A. A. K. BOOTH
CARL G. PAULSEN
LLOYD D. KNAPP
GLENN W. HOLCOMB
FRANCIS M. DAWSON

Term expires October, 1956:
WILLIAM S. LaLONDE, JR.
OLIVER W. HARTWELL
THOMAS C. SHEDD
SAMUEL B. MORRIS
ERNEST W. CARLTON
RAYMOND F. DAWSON

Term expires October, 1957:
JEWELL M. GARRELTS
FREDERICK H. PAULSON
GEORGE S. RICHARDSON
DON M. CORBETT
GRAHAM P. WILLOUGHBY
LAWRENCE A. ELSENER

PAST-PRESIDENTS

Members of the Board

WALTER L. HUBER
DANIEL V. TERRELL

EXECUTIVE SECRETARY

WILLIAM N. CAREY

ASSOCIATE SECRETARY

WILLIAM H. WISELY

TREASURER

CHARLES E. TROUT

ASSISTANT SECRETARY

E. L. CHANDLER

ASSISTANT TREASURER

CARLTON S. PROCTOR

PROCEEDINGS OF THE SOCIETY

HAROLD T. LARSEN
Manager of Technical Publications

DEFOREST A. MATTESON, JR.
Editor of Technical Publications

PAUL A. PARISI
Assoc. Editor of Technical Publications

COMMITTEE ON PUBLICATIONS

SAMUEL B. MORRIS, *Chairman*

JEWELL M. GARRELTS, *Vice-Chairman*

GLENN W. HOLCOMB
OLIVER W. HARTWELL
ERNEST W. CARLTON
DON M. CORBETT